*Pol. J. Environ. Stud. Vol. XX, No. X (XXXX), 1-9*

DOI: *10.15244/pjoes/213854* ONLINE PUBLICATION DATE: 2025-12-22

*Original Research*

# Molecular Weight- and Type-Dependent Heterogeneity in Dissolved Organic Matter Binding with Heavy Metals in Natural Waters

**TianBao Guo[1], Huacheng Xu[2]***

[1]Zhou Enlai School of Government and Management, Nankai University, Tianjin, China
[2]Key Laboratory of Lake and Watershed Science for Water Security, Nanjing Institute of Geography and Limnology, Chinese Academy of Sciences, Nanjing, China

*Received: 13 August 2025*
*Accepted: 2 November 2025*

## Abstract

Dissolved organic matter (DOM) in aquatic ecosystems can bind with heavy metals, which substantially affects the behavior and fate of the metals. However, the binding potential is highly related to the molecular weights and types of the DOM samples. In this study, aquatic DOMs from different ecosystems (i.e., river and lake) were fractionated into low molecular weight (LMW-, <1 kDa) and high molecular weight (HMW-, 1 kDa~0.45 μm) fractions, and the MW-dependent heterogeneities in Cd(II) were investigated by spectral and titration techniques. The results showed that 38.1~40.1% of organic ligands were distributed in the LMW-fraction, with the remaining 59.9~61.9% in the HMW-fraction. Parallel factor analysis identified one tryptophan-, one tyrosine-, and one fulvic-like component from 60 pristine fluorescence spectra. It was noted that the tryptophan- and tyrosine-like components were mainly located in the HMW-fraction, while the fulvic-like components became the predominant organic ligands in the LMW-fraction. Fluorescence titration analysis showed that, with increased metal addition, the intensities of all fluorescent components exhibited an initial rapid decline followed by a gradual decrease or stabilization, demonstrating effective binding of heavy metals with DOMs. The modified Stern-Volmer model further demonstrated that the Cd(II) binding potential ($logK_M$) of river DOMs was generally lower than that of lake DOMs for each MW fraction. In addition, irrespective of DOM types, the $logK_M$ values decreased with the order of HMW- > Bulk > LMW-, showing obvious MW-dependent heterogeneities in metal binding. This study clearly revealed that the binding properties of heavy metals with natural DOMs were highly dependent on DOM types as well as MWs.

**Keywords**: aquatic DOMs, DOM types, molecular weight, heavy metal binding, fluorescence titration

---

*e-mail: hcxu@niglas.ac.cn
ORCID iD: 0000-0003-1724-6720

## Introduction

Dissolved organic matter (DOM), which consists of various organic components (e.g., humic acids, proteins, and carbohydrates) and a wide range of molecular sizes (<1 kDa~0.45 μm), is ubiquitous in aquatic environments [1, 2]. DOM in natural waters plays a critical role in balancing and structuring ecosystems, and its degradation process can significantly affect carbon emissions and mass circulation [3]. Owing to the presence of multiple active sites, aquatic DOMs can also complex and chelate heavy metals, thereby influencing the behavior, fate, and bioavailability of these heavy metals [4, 5].

Metal binding with DOM has been widely studied in many aquatic environments, including sloughs [6], lakes [7], soils [8, 9], sediments [10, 11], sludge [12], and algal exudates [13]. It was reported that humic-like substances in sloughs exhibited a high Cu(II) binding potential, with a conditional stability constant ($logK_M$) of 4.5~6.3 [6], while in reservoirs and river waters, the concentrations of Cu(II) did not show a strong correlation with the number of active sites in humic-like substances [14]. In addition, protein-like components within autochthonous DOMs showed high binding potential with Cu(II), but the humic-like substances became important chelates for allochthonous DOMs [5]. These heterogeneities indicated that the metal-DOM interaction was highly dependent on the sources and types of DOM samples. A comparison of metal-binding heterogeneities between river and lake waters can reveal source-dependent heterogeneities in DOM samples and is, more importantly, of considerable importance for gaining a deeper insight into the behavior and fate of heavy metals along the river-lake transect. Furthermore, previous studies on metal-DOM interaction have focused mainly on bulk DOM samples, lacking binding information on heavy metals with molecular weight (MW)-fractionated DOMs [15]. In fact, aquatic DOM samples are characterized by a wide range of molecular sizes from <1 kDa to 0.45 μm [16, 17], and different MW-fractionated DOM would exhibit distinct binding affinities toward heavy metals due to their differing components and functional groups. To the best of our knowledge, information on MW-dependent heterogeneities in metal binding with DOM between river and lake waters has not yet been reported.

Aquatic DOMs can fluoresce in nature, and some spectral methods, such as fluorescence emission-excitation matrix combined with parallel factor (EEM-PARAFAC) analysis, can thus be used to reveal the inherent organic components [18, 19]. In addition, it is well known that the fluorescent components in DOMs can be quenched by metals via static and/or dynamic quenching [5, 6, 20]. Thus, the metal binding parameters of MW-fractionated DOMs between river and lake waters can be efficiently revealed by the fluorescence quenching technique combined with EEM-PARAFAC analysis.

The objectives of this study were to: 1) compare the MW-dependent concentrations and compositions of natural DOMs from different sources; 2) characterize the metal-binding behaviors of DOMs in terms of MWs and organic components; and 3) reveal the MW-dependent binding heterogeneities of these natural DOM samples. For this reason, river and lake waters were sampled and fractionated into low MW- (LMW-, <1 kDa) and high MW- (HMW-, 1 kDa~0.45 μm) fractions, respectively. The heavy metal Cd(II) was applied as the representative heavy metal due to its high biotoxicity in aquatic environments [21]. Fluorescence quenching combined with EEM-PARAFAC was applied to reveal the MW-dependent binding properties of DOMs from different sources. The results obtained can deepen our understanding of the importance of MWs of DOMs in metal binding and the behavior and fate of heavy metals in aquatic environments, especially along river-lake transects.

## Materials and Methods

### Sampling of Water Samples

River waters were sampled from the Nanjing region of the Yangtze River, the largest and longest river in China. The lake waters were collected from Meiliang Bay of Lake Taihu, which is one of the largest lakes in China. After collection, both the river and lake samples were stored at 4°C in the dark, transported to the lab as soon as possible, and then filtered through a 0.45 μm membrane to obtain the DOM samples.

### Molecular Weight-Dependent Fractionation of DOMs

The stirred-cell ultrafiltration system (Amicon, USA), equipped with a 1 kDa membrane disc (Millipore, PLAC07619), was used to obtain the MW-fractionated DOM samples. Before ultrafiltration, the membrane discs were cleaned repeatedly using HCl (0.02 M) and NaOH (0.05 M) solutions, followed by flushing with ultrapure water. For each ultrafiltration, 300 mL of bulk DOM samples were transferred to the stirred cell that was preloaded with membrane discs [2]. The ultrafiltration system was carried out under a nitrogen pressure of 345 kPa and a concentration factor of 30 with continuous stirring. The permeate solutions represented the organic ligands with MW<1 kDa, whereas the retentates were diluted to 300 mL and regarded as the HMW fraction (1 kDa~0.45 μm) [2, 16].

### Binding of Heavy Metals with Molecular Weight-Dependent DOM

The titration experiments were conducted to examine the binding properties of the bulk and MW-fractionated DOM samples with Cd(II) in duplicate. Specifically, 0.1 M Cd(II) solutions were added to a series of vials containing 50 mL of bulk or MW-fractionated DOM solution using an automatic syringe [6, 18, 22]. The concentrations of Cd(II) in the final solutions varied in the range of 5 to 100 μM via the addition of no more than 50 μL of titrant. Based on the Visual MINTEQ analysis, all titrated solutions were adjusted to pH 6.0~6.2, under which no precipitate was formed [18]. After metal addition, the mixtures were shaken immediately and then stored at room temperature in the dark for 24 h to ensure reaction equilibrium, followed by the fluorescence spectral determination [5, 6].

### Quantitative Calculation of the Binding Potential of Heavy Metals with DOMs

The modified Stern-Volmer model was used to quantify the binding potential of metals with individual organic ligands, including the bulk and MW-fractionated components, and expressed as follows:

$$\frac{F_o}{F_o - F} = \frac{1}{f \cdot K_M \cdot C_M} + \frac{1}{f} \tag{1}$$

where $F$ and $F_0$ are the intensities of fluorescent components with and without metal addition; $K_M$ is the conditional stability constant, which can be obtained by plotting $F_0/(F_0-F)$ against $1/C_M$; and $f$ represents the fraction of the initial organic ligands that correspond to metal binding [20].

### Other Analytical Methods

Concentrations of DOC in the bulk and MW-fractionated DOM samples were measured using a TOC analyzer (Shimadzu, TOC-L). UV-Vis absorption spectra were obtained using a spectrophotometer (UV-2550, Shimadzu), at wavelengths in the range of 200~800 nm with 1 nm increments. Fluorescence emission-excitation matrix (EEM) spectra were collected at emission (Em) wavelength 250~550 nm and excitation (Ex) wavelength 200~500 nm using a Hitachi F-7000 spectrofluorometer (Tokyo, Japan). The increments of Em and Ex wavelengths were 2 nm and 10 nm, respectively. The spectrum of ultrapure water was recorded at intervals of 10 analyses to ensure no contamination, and interferences from first and second scatter peaks were eliminated accordingly [6, 14].

PARAFAC is a generalization of bilinear principal component analysis to higher-order arrays, which statistically decomposes three-way data into individual fluorescence components. Each fluorophore gives rise to one PARAFAC component, and the scores of components can be used to indicate the relative concentration of different fluorophores. The PARAFAC model in this study was carried out using MATLABR2013a and the freely available DOMFluor toolbox (http://www.models.life.ku.dk). After several post-acquisition steps for the pristine EEM spectra, the PARAFAC model with two to seven components was computed, with the correct component numbers validated by the residual analysis, split-half analysis, as well as visual inspection [5, 6].

## Results and Discussion

### Molecular Weight-Dependent Heterogeneities in Concentrations and Properties of DOM Samples

Fig. 1 compares the MW-dependent heterogeneities in the concentrations and spectral properties of river and lake DOMs. The DOC concentrations for the bulk river and lake DOMs were 5.36 mg $L^{-1}$ and 12.31 mg $L^{-1}$, respectively, and those for the LMW fractions were 2.15 mg $L^{-1}$ and 4.69 mg $L^{-1}$, respectively. The results demonstrated that 40.1% of river organic ligands and 38.1% of lake organic substances were distributed in the LMW fraction. The distribution percentage of LMW fractions observed herein was generally lower than in other oligotrophic aquatic waters, such as ~70% in Lake Michigan [2], 80% in rivers of Siberia [23], >60% in the Mississippi River [24], and ~77% in seawater [2]. These results indicate that the MW-dependent abundance heterogeneities of natural DOMs may be related to the eutrophic states of aquatic ecosystems.

The absorption spectra for all bulk and MW-fractionated samples exhibited similar patterns, in which the absorbance decreased quasi-exponentially with increasing wavelength. Further analysis showed that the HMW fraction possessed higher absorbance than the bulk and LMW fractions, irrespective of DOM types. The results indicate that the aromatic substances in the river and lake DOM pools were mainly distributed in the HMW fraction [25].

### Fluorescence EEM Spectra of the River and Lake DOM Samples

To compare the organic components between the river and lake DOM samples, fluorescence spectroscopy was applied herein. As depicted in Fig. 2, both the river and lake DOM samples were characterized by four main peaks, i.e., peak A (Em/Ex: 340/230 nm), peak B (Em/Ex: 320/280 nm), peak C (Em/Ex: 450/230 nm), and peak D (Em/Ex: 420/320 nm). Peaks A and B were ascribed to tyrosine- and tryptophan-like fluorophores, respectively, whereas peaks C and D can be assigned to fulvic- and humic-like fluorophores [15]. The EEM results revealed the complex nature of eutrophic river and lake DOMs in which protein-, humic-, and fulvic-like fluorophores coexisted within the DOM pools, a pattern also observed in other natural DOMs [18]. Further analysis showed that tyrosine- and tryptophan-like substances exhibited higher fluorescence intensities than the humic- and fulvic substances for lake DOM,

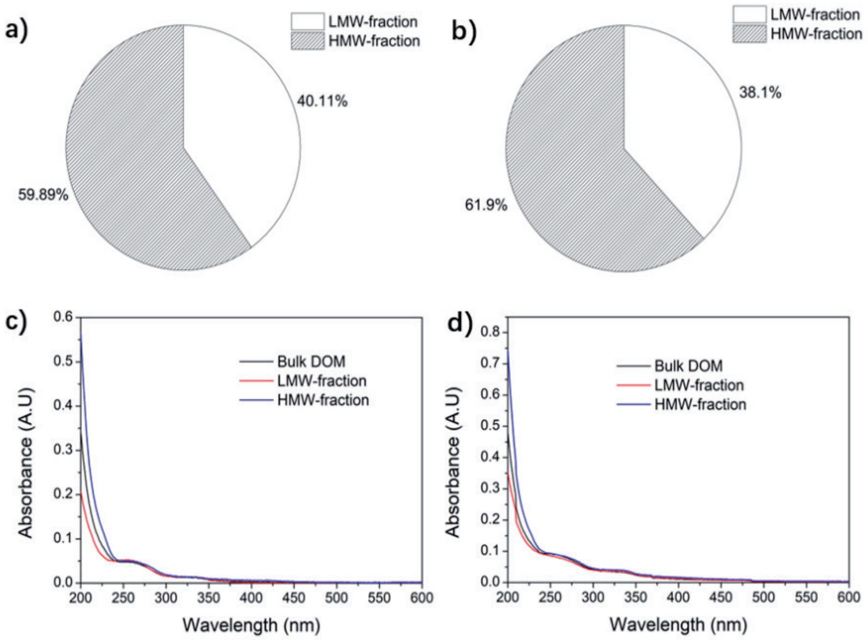

Fig. 1. MW-dependent heterogeneities in DOC abundance and spectral properties of river (a, c) and lake (b, d) DOM samples.

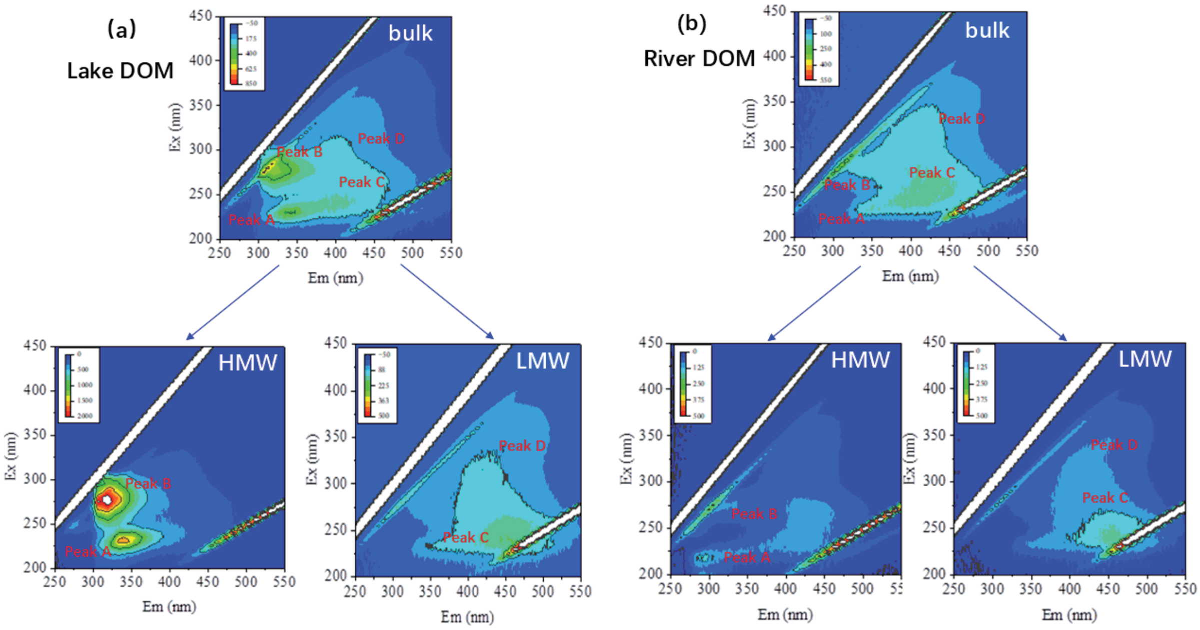

Fig. 2. MW-dependent heterogeneities in fluorescence spectra of DOMs from different origins. a) Lake DOM; b) River DOM.

while the reverse pattern was found for river DOM. This result indicates the allochthonous origins of DOMs in river samples and the autochthonous properties of DOMs in lake samples.

As for the MW-dependent distribution properties, it was found that peaks A and B were located in the HMW fraction, while peaks C and D became the main fluorophores in the LMW counterparts, irrespective of DOM types. This indicated that protein-like substances were mainly located in the HMW fraction, whereas humic- and fulvic-like substances were predominantly distributed in the LMW fraction. The distribution of organic components among different MW fractions observed herein was similar to that of sedimentary DOMs, model DOMs, and algal exudates [15, 26], indicating that the MW-related distribution patterns were independent of DOM types. Compared with the humic- and fulvic-like substances, the aromatic protein-like ligands were prone to self-aggregate, forming large molecular-size aggregates [27], which were responsible for their predominant distribution within the HMW fraction.

## PARAFAC Analysis of the Fluorescence EEM Spectra

Although fluorescence EEM spectroscopy can effectively track the abundance of organic components, the pristine EEM spectra usually suffer from an obvious peak-overlapping problem. In order to enhance spectral resolution and, more importantly, to identify the independent organic components, PARAFAC analysis was applied to decompose the pristine EEM spectra. A total of 60 pristine EEM spectra were used for the PARAFAC analysis. Based on the residual analysis, a three-component model was used to decompose the pristine EEM spectra (Fig. 3).

Component 1 (C1) exhibited two peaks at Em/Ex of 340/230 and 340/280 nm, respectively, which can be ascribed to a tryptophan-like component [16]. C2 was characterized by a peak at Em/Ex of 320/280 nm and can be classified as a tyrosine-like component. C3 contained a primary peak (Em/Ex = 450/230 nm) and a secondary peak (Em/Ex = 470/340 nm) and was identified as a fulvic-like component [22]. These similar fluorescent components have been previously found in some sedimentary DOMs [10] and other surface waters, such as river waters, lake waters, and seawater [2].

## Binding Behavior of PARAFAC-Derived Components in Response to Cu(II) Addition

Fig. 4 delineates the variations in fluorescence intensities of the three PARAFAC-derived components in response to metal addition. With increasing metal addition (0~100 μM), all fluorescent components exhibited an initial rapid decrease followed by a gradual decline or stabilization, indicating effective binding of the DOM samples with metals [18]. The ground-state fluorescent substances within the DOM pool can bind with metal quenchers through weak interactions such as van der Waals forces and hydrogen bonds, forming nonfluorescent complexes that cause the decline

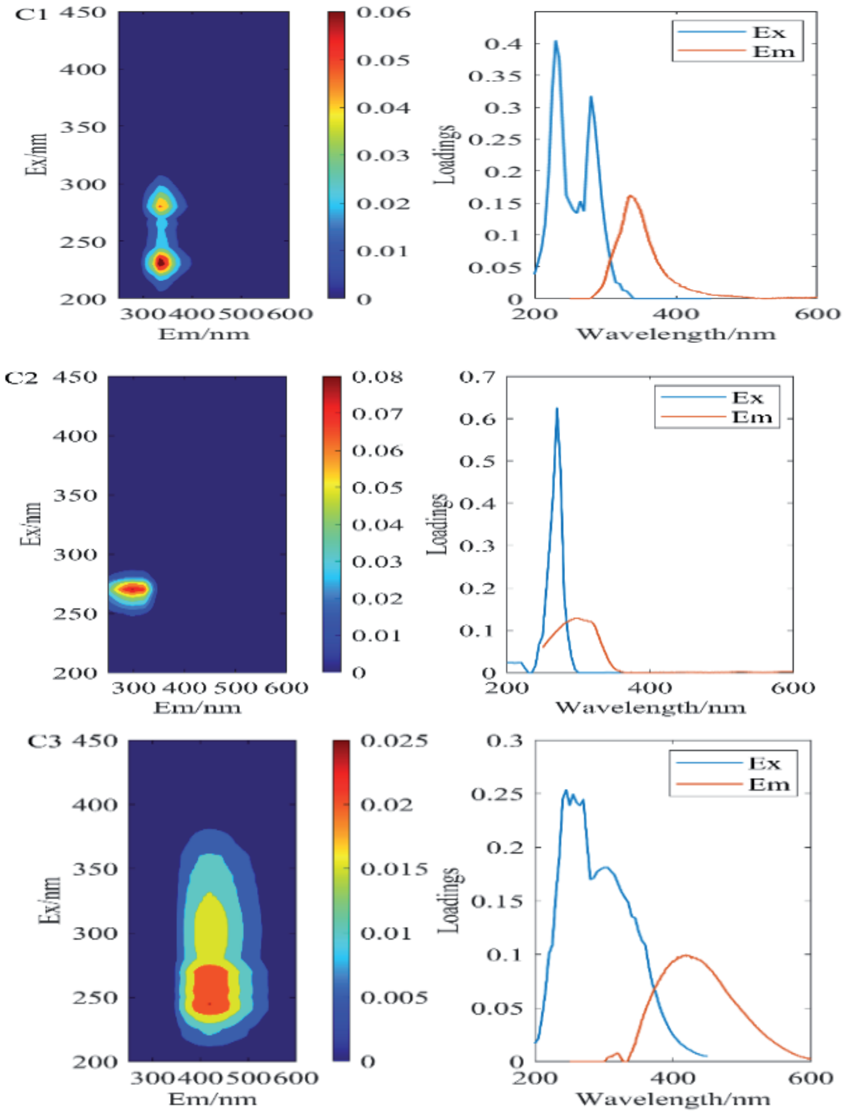

Fig. 3. The EEM contours and Em/Ex loadings of the three fluorescent components derived from the PARAFAC model.

in fluorescence intensity. Further data analysis showed that the quenching extents of fluorescent components exhibited obvious differences that were highly related to DOM types and MWs. For example, with increasing metal addition, the intensities of C1 and C2 in the two DOM samples decreased by 52.8~57.8%, while those of C3 decreased by 60.0~67.0%, indicating more effective binding of humic- and fulvic-like components with metals. In addition, irrespective of DOM types, the percentage decrease in fluorescence intensity followed the order of 66.4~79.8% for HMW fraction > 52.8~67.0% for bulk fraction > 49.7~62.1% for the LMW fraction, demonstrating that the HMW organic ligands exhibited the highest binding efficiencies, followed by the bulk and then the LMW organic ligands. This can be ascribed to the different organic components and binding sites between the LMW and HMW fractions.

It was noted that the intensity of fluorescent substances was either enhanced or quenched with increasing metal addition, depending on the metal types, fluorescence components, and experimental conditions [20]. Metal-induced fluorescence enhancement has been widely reported in previous studies focusing on sedimentary DOM [11] and natural DOM [6]. Compared with previous studies, the phenomenon of fluorescence enhancement was not observed in this study, indicating the absence of changes in the molecular environments of these organic molecules during metal addition. The quenching mechanisms of organic ligands with metal addition include both dynamic and static quenching. Static quenching occurs when the quencher coordinates with the fluorescent group to form a nonfluorescent complex, whereas dynamic quenching occurs through interactions between the quencher and the excited-state molecules of the fluorophore [20]. In this study, changes in absorption spectra and time-resolved fluorescence identified static quenching as the main quenching mechanism.

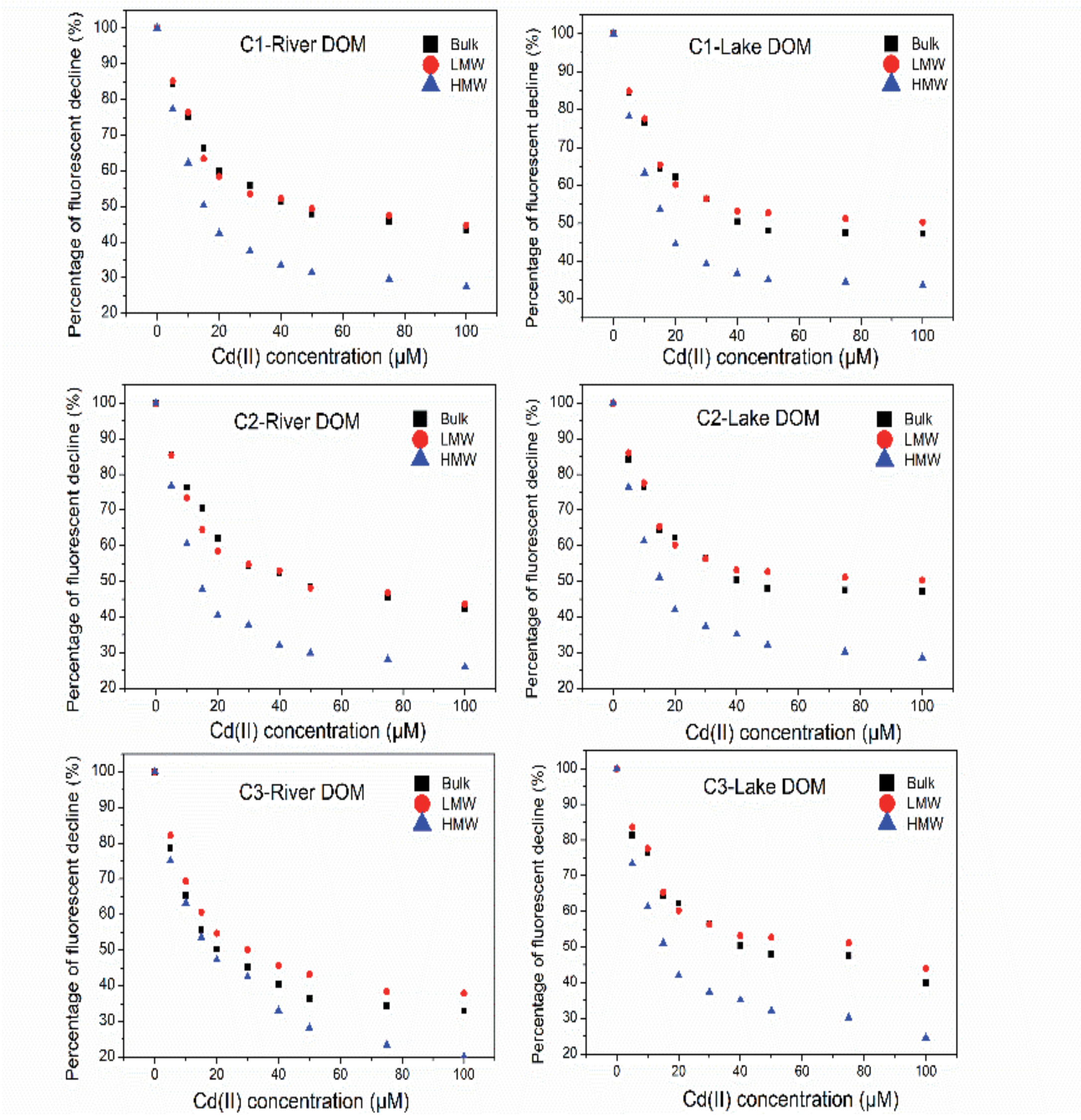

Fig. 4. Variations in fluorescence intensities in response to metal addition.

Table 1. MW-dependent binding properties of Cd(II) with river and lake DOMs.

| Components | MWs | River DOM | | Lake DOM | |
|---|---|---|---|---|---|
| | | $LogK_M$ ($R^2$) | f | $LogK_M$ ($R^2$) | *f* |
| C1 | Bulk | 4.77 (0.996) | 0.693 | 4.78 (0.986) | 0.675 |
| | LMW- | 4.71 (0.982) | 0.731 | 4.79 (0.976) | 0.642 |
| | HMW- | 4.83 (0.988) | 0.913 | 4.85 (0.983) | 0.854 |
| C2 | Bulk | 4.72 (0.996) | 0.703 | 4.79 (0.985) | 0.667 |
| | LMW- | 4.70 (0.984) | 0.745 | 4.72 (0.978) | 0.683 |
| | HMW- | 4.83 (0.983) | 0.935 | 4.87 (0.989) | 0.878 |
| C3 | Bulk | 4.87 (0.996) | 0.802 | 4.90 (0.957) | 0.622 |
| | LMW- | 4.78(0.992) | 0.778 | 4.83 (0.970) | 0.628 |
| | HMW- | 4.90 (0.994) | 0.865 | 4.97 (0.994) | 0.831 |

### Molecular Weight-Dependent Heterogeneities in Binding Properties of DOMs from Different Origins

The modified Stern-Volmer model was applied to reveal the MW-dependent binding behaviors of individual fluorescent components with metals (Table 1). The calculated conditional stability constant ($LogK_M$) values for the three fluorescent components ranged from 4.71 to 4.85 for C1, 4.70 to 4.87 for C2, and 4.78 to 4.97 for C3, respectively, which were of the same order of magnitude as those found for sedimentary DOMs [5], sludge extracellular polymeric substances [12], and landfill leachates [4]. Further data analysis showed that these organic ligands were characterized by varied binding potential that was highly related to the organic components and MWs. For instance, the $LogK_M$ values for river samples were generally lower than those for lake samples, irrespective of organic components and DOM types, indicating a low metal-binding potential for river DOMs. The reason may be attributed to generally higher ionic strengths in river waters, which can compete with heavy metals for the binding sites. It was also shown that the $LogK_M$ values for the HMW-fraction (4.83~4.97) were generally higher than the bulk (4.72~4.90) and the LMW-fraction (4.70~4.83), regardless of organic components and DOM types. The results agree with previous studies showing higher metal-binding potential for organic ligands with large molecular sizes [15]. Compared with the LMW-fraction, the HMW counterparts exhibited higher absorbance and aromaticity (C=O and C=C double bonds) (Fig. 1), which corresponded to higher binding strength [28], accounting for the higher $LogK_M$ values observed.

The *f* values of fluorescent components for the bulk samples ranged from 0.693 to 0.802 for river DOMs and 0.622 to 0.675 for lake DOMs, indicating a high abundance of binding sites for heavy metals. It was noted that the *f* values observed herein were significantly higher than those reported in previous studies investigating sedimentary DOM (0.12~0.69) [15]. Further data analysis showed that, regardless of organic components and DOM types, the *f* values of the HMW fraction were always higher than those of the LMW counterparts, indicating that the binding sites of DOMs with heavy metals were also MW-dependent.

Lastly, our results showed significant environmental implications for river-lake management and ecological restoration. For example, this study found higher metal-binding capacities for river DOMs than for lake samples. Since the bioavailability of heavy metals is highly related to the free ion forms [6], the biotoxicity of heavy metals in river waters should receive more attention, as the river waters often flow into lakes. This accounts for the fact that river waters can usually be considered a pollutant source in terms of heavy metals due to their low metal-binding potential and high abundance of free-ion forms [29]. In addition, due to the ubiquitous heavy metal pollution in river, lake, and estuarine ecosystems, the application of biological chelating agents has been widely reported as an effective technology [30]. Our results demonstrated that the HMW organic ligands exhibited higher metal-binding capacities than the LMW counterparts, suggesting that some HMW chelating agents, such as glutamic acid, ethylenediaminetetraacetic acid, and S,S-ethylenediamine-disuccinate-derived chelators [31, 32], can be prioritized for the detoxification of heavy metals. In addition, ecological restoration (e.g., phytoremediation) is a widely used technology for polluted sediments [33]. Since plant root exudates consist of various organic compounds and multiple functional groups that can effectively bind with heavy metals to reduce biotoxicity [34], plant species characterized by a high abundance of root exudates are proposed, based on our results, for their high metal-binding potential.

## Conclusions

In this study, fluorescence spectroscopy, metal titration, and ultrafiltration procedures were applied to explore the MW- and type-dependent binding properties of heavy metals with natural DOMs. Irrespective of DOM types, most organic ligands, especially the tryptophan- and tyrosine-like components, were distributed within the HMW fraction. For each MW fraction, the $logK_M$ values for river DOMs were generally lower than those for lake DOMs. In addition, regardless of DOM types, the $logK_M$ values decreased in the order of: HMW- > Bulk > LMW-. Our results demonstrated that metal binding with DOMs in natural waters was MW- and type-dependent, which can provide valuable theoretical guidance for river-lake management and ecological restoration. Further studies should measure *in situ* variations in the distribution, speciation, and bioavailability of heavy metals along the river-lake transect.

## Acknowledgements

This work was supported by the National Natural Science Foundation of China (52525904, 52479079), the Key Research and Development Program of Jiangsu Province (BE2023846), and the Natural Science Foundation of Qinghai Province, China (2024-ZJ-936).

## Conflict of Interest

The authors declare no conflict of interest.

## References

1. D'ANDRILLI J., SILERMAN V., BUCKLEY S., ROSAROP-ORTIZ F.L. Inferring ecosystem function from dissolved organic matter optical properties: A critical review. Environmental Science & Technology. **56**, 11146, **2022**.
2. XU H.C., GUO L.D. Molecular size-dependent abundance and composition of dissolved organic matter in river, lake and sea waters. Water Research. **117**, 115, **2017**.
3. YOU J.K., LIU F., WANG Y.W., DUAN C.S., ZHANG L., LI H.S., WANG J.J., XU H.C. Photo-methanification of aquatic dissolved organic matters with different origins under aerobic conditions: Non-negligible role of hydroxyl radicals. Water Research. **256**, 121609, **2024**.
4. NGUGYN T.N., TAKAOKA M., KUSAKABE T., SHITO K. Assessing the complexation of dissolved organic matter with heavy metals ($Cu^{2+}$, $Pb^{2+}$) in leachate from an old Japanese landfill site using fluorescence quenching. Environmental Science and Pollution Research. **31** (39), 52253, **2024**.
5. XU H.C., GUAN D.X., ZOU L., LIN H., GUO L.D. Contrasting effects of photochemical and microbial degradation on Cu(II) binding with fluorescent DOM from different origins. Environmental Pollution. **239**, 205, **2018**.
6. YAMASHITA Y., JAFFE R. Characterizing the interactions between trace metals and dissolved organic matter using excitation-emission matrix and parallel factor analysis. Environmental Science & Technology. **42**, 7374, **2008**.
7. YANG K.L., ZHANG Y.L., PENG J.Y., XU H.C., LIU X., LIU H.N., LI N., GUO L.D., LI W. Molecular weight-dependent differences in spectral properties and metal-binding behaviors of dissolved organic matter from different lakes. Science of The Total Environment. **946**, 174245, **2024**.
8. CHEN W., LI P., HU K.R., ZHANG Z., PENG C.H., TENG C.Y., ZHOU K.G. Spectroscopic response of soil organic matter in mining area to Pb/Cd heavy metal interaction: A mirror of coherent structural variation. Journal of Hazardous Materials. **393**, 122425, **2020**.
9. LIN W., GUO X.L., WANG Y.L., ZHAO J.L., CHENG X., LI Y.J., ZHOU C.Y. Dissolved organic matter mediates the interactions between bacterial community and heavy metal fractionation in contaminated coal mine soils. Ecotoxicology and Environmental Safety. **297**, 118237, **2025**.
10. LIU Y.M., LI M.Y., REN D., LI Y.X. Spatial distribution of sediment dissolved organic matter in oligotrophic lakes and its binding characteristics with Pb(II) and Cu(II). Environmental Science and Pollution Research. **31**, 43369, **2024**.
11. LÜ W.W, YAO X., REN H.Y., DENG H.G., YAO M., ZHANG B.H. Characterizing the interactions between sediment dissolved organic matter and zinc using multispectroscopic techniques. Environmental Pollution. **261**, 113644, **2020**.
12. YESIL H., MOLARY R., CALLI B., TUGTAS A.E. Extent of bioleaching and bioavailability reduction of potentially toxic heavy metals from sewage sludge through pH-controlled fermentation. Water Research. **201**, 117303, **2021**.
13. GARRAUD J., PLIPHON H., CAPIAUX H., LE GUERN C., MENCH M., LEBEAU T. Drivers to improve metal (loid) phytoextraction with a focus on microbial degradation of dissolved organic matter in soils. International Journal of Phytoremediation. **26** (1), 63, **2024**.
14. YAN M.Q., MA J., ZHANG C.Y., ZHOU Y.X., LIU F., HAN X.Z., LI M.Y., NI J.R. Optical property of dissolved organic matters (DOMs) and its link to the presence of metal ions in surface freshwaters in China. Chemosphere. **188**, 502, **2017**.
15. XU H.C., ZOU L., GUAN D.X., LI W.T., JIANG H.L Molecular weight-dependent spectral and metal binding properties of sediment dissolved organic matter from different origins. Science of the Total Environment. **665**, 828, **2019**.
16. XU H.C., GUO L.D. Intriguing changes in molecular size and composition of dissolved organic matter induced by microbial degradation and self-assembly. Water Research. **135**, 187, **2018**.
17. SANTSCHI P.H. Marine colloids, agents of the self-cleansing capacity of aquatic systems: Historical perspective and new discoveries. Marine Chemistry. **207**, 124, **2018**.
18. HE C.J., LIU N.N., MENG W., LI Z.F. Characterization of metal-binding behavior of DOM component structure in biochar: Analysis of binding sites, binding sequences and impact pathways. Journal of Environmental Chemical Engineering. **12**, 113861, **2024**.

19. YANG L.Y., CHEN L.W., ZHUANG W.E., ZHU Z.Y. Unveiling changes in the complexation of dissolved organic matter with Pb(II) by photochemical and microbial degradation using fluorescence EEMs-PARAFAC. Environmental Pollution. **341**, 122982, **2024**.
20. LI W.J., LU L., DU H.H. Deciphering DOM-metal binding using EEM-PARAFAC: Mechanisms, challenges, and perspectives. Environmental Science and Pollution Research. **31**, 14388, **2024**.
21. MOISEENKO T.I., GASHIKINA N.A. Distribution and bioaccumulation of heavy metals (Hg, Cd and Pb) in fish: Influence of the aquatic environment and climate. Environmental Research Letters. **15** (11), 115013, **2020**.
22. WANG X.H., ZOU T.S., ZHANG W.B., FAN Y.L., BAI Y.C. Vertical binding characteristics between dissolved organic matter and heavy metals in the upper reaches of the Yangtze river using EEM-PARAFAC and 2D-FTIR-COS. Water. **17** (9), 1359, **2025**.
23. POKROVSKY O.S., MANASYPOV R.M., LOIKO S.V., SHIRIKIVA L.S. Organic and organo-mineral colloids in discontinuous permafrost zone. Geochimica Cosmochimica Acta. **188**, 1, **2016**.
24. CAI Y.H., GUO L.D., WANG X.R., AIKEN G. Abundance, stable isotopic composition, and export fluxes of DOC, POC, and DIC from the Lower Mississippi River during 2006-2008. Journal of Geophysical and Research: Biogeosciences. **120** (11), 2273, **2015**.
25. LEE Y.K., LEE M.H., HUR J. A new m olecular weight (MW) descriptor of dissolved organic matter to represent the MW-dependent distribution of aromatic condensation: Insights from biodegradation and pyrene binding experiments. Science of The Total Environment. **660**, 169, **2019**.
26. XU H.C., LI F.F., KONG M., LV X.Z., DU H.Y., JIANG H.L. Adsorption of cyanobacterial extracellular polymeric substance on colloidal particle: Influence of molecular weight. Science of the Total Environment. **715**, 136959, **2020**.
27. ZHOU D.D, ZHANG C.F, FU L., XU L., CUI X.C., LI Q.C, CRITTENDEN J.C. Responses of the microalga Chlorophyta sp. to bacterial quorum sensing molecules (N-acylhomoserine lactones): aromatic protein-induced self-aggregation. Environmental Science & Technology. **51** (6), 3490, **2017**.
28. HUANG M., LI Z.W., LUO N.N., YANG P., WEN J.J., HUANG B., ZENG G.M. Application potential of biochar in environment: Insight from degradation of biochar-derived DOM and complexation of DOM with heavy metals. Science of the Total Environment. **646**, 220, **2019**.
29. XIA F., QU L.Y., WANG T., LUO L.L., CHEN H., DAHLGREN R.A., ZHANG M.H., MEI K., HUANG H. Distribution and source analysis of heavy metal pollutants in sediments of a rapid developing urban river system. Chemosphere. **207**, 218, **2018**.
30. KHARE S., SINGHAL A., RALLAPALLI S., MISHRA A. Bio-chelation for sustainable heavy metal remediation in municipal solid waste compost: A critical review of chelation technologies. Environmental Science and Pollution Research. 1, **2025**.
31. SUANON F., SUN Q., DIMON B., MAMA D., YU C.P. Heavy metal removal from sludge with organic chelators: comparative study of N, N-bis (carboxymethyl) glutamic acid and citric acid. Journal of Environmental Management. **166**, 341, **2016**.
32. ULLMANN A., BRAUNER N., VAZANA S., KATZ Z., GOIKHMAN R., SEEMANN B., MAROM H., GOZIN M. New biodegradable organic-soluble chelating agents for simultaneous removal of heavy metals and organic pollutants from contaminated media. Journal of Hazardous Materials. **260**, 676, **2013**.
33. PENG W.H., LI X.M., XIAO S.T., FAN W.H. Review of remediation technologies for sediments contaminated by heavy metals. Journal of Soils and Sediments. **18** (4), 1701, **2018**.
34. ULBRICH T.C., RIVAS-UBACH A., TIEMANN L.K., FRIESEN M.L., EVANS S.E. Plant root exudates and rhizosphere bacterial communities shift with neighbor context. Soil Biology and Biochemistry. **172**, 108753, **2022**.